

Seismic Behaviour of Masonry Arches with Tie-Rods: Dynamic Tests on a Scale Model

C. Calderini, S. Lagomarsino & M. Rossi

University of Genoa, Italy

G. Decanio, M.L. Mongelli & I. Roselli

ENEA MAT-QUAL, Casaccia, Rome, Italy



SUMMARY:

In arches and vaults, tie-rods play a decisive role in the control of horizontal thrusts produced by both permanent and seismic loadings. For these reasons, still today tie-rods are widely used as reliable technique for the reinforcement of masonry buildings. Usually, steel bars similar in size and shape to ancient ones and fixed to stonework by means of bolts or plates are adopted. However, some innovative solutions to improve the technique were recently proposed. The common aim of such solutions is to increase the displacement capacity and dissipation of the arch-pillars-rod system under seismic actions. In this paper, the effectiveness of flexible tie-rods to improve the seismic response of arch-pillars system is assessed by mean of shaking table tests and simple analytical models developed in the framework of performance-based design.

Keywords: Masonry Arches, Shaking Table Tests, Displacement Capacity

1. MOTIVATION AND AIMS

In historic masonry buildings, tie-rods contribute to guaranteeing an efficient connection between the constituting parts of the structure. In particular, in arches and vaults, such elements play a decisive role in the control of horizontal thrusts produced by both permanent and seismic loadings. In particular, tie-rods couple the displacement of springing of arches (or top of pillars), inhibiting the formation of typical 5-hinges symmetric and 4-hinges asymmetric collapse mechanisms. For these reasons, still today tie-rods are widely used as reliable technique for the reinforcement of masonry buildings (replacement of broken/damaged tie-rods or introduction of new ones). Usually, steel bars similar in size and shape to ancient ones and fixed to stonework by means of bolts or plates are adopted. However, some innovative solutions to improve the technique were recently proposed. The common aim of such solutions is to increase the displacement capacity and dissipation of the arch-pillars-rod system under seismic dynamic actions.

In this paper, the behaviour of arch-piers systems reinforced with different types of tie-rods is analyzed by presenting the results of an experimental campaign carried out on a scale model at ENEA MAT-QUAL laboratory in Casaccia (Rome) and by interpreting them through simple analytical models developed in the framework of displacement-based design methods. The research work had two aims. On the one hand, the influence of the stiffness of tie-rods on arch-piers systems is analysed. On the other hand, the reliability of a displacement-based procedure of analysis developed by the authors for masonry structures subjected to rigid blocks collapse mechanisms (Lagomarsino and Resemini, 2009) is assessed.

In the procedure proposed, the structure is first reduced to a SDOF mechanism constituted by the rigid motion of n blocks subjected to their weight W_i and proportional horizontal forces αW_i . The collapse multiplier α that induces loss of equilibrium of the system is then calculated for increasing finite values of the generalized coordinate ξ of the considered DOF, up to the value for which $\alpha(\xi_u)=0$. The

capacity curve of the system is finally defined by converting it in an equivalent non-linear SDOF system, whose principal mode of vibration is consistent with the mechanism considered. Its seismic spectral acceleration a^* may be thus calculated as:

$$a^*(\xi) = \alpha(\xi) \frac{\sum_{i=1}^n W_i}{M^*} \quad (1.1)$$

where W_i is the weight of the i -th block and M^* is mass of the structure participating in the mechanism, that can be calculated as:

$$M^* = \frac{\left(\sum_{i=1}^n W_i \delta_{x,i} \right)^2}{g \sum_{i=1}^n W_i \delta_{x,i}^2} \quad (1.2)$$

g being the gravity acceleration and $\delta_{x,i}$ being the horizontal virtual displacement of the centroid of the i -th block calculated with reference to the initial configuration of the system.

The spectral displacement may be calculated as:

$$d_x^*(\xi) = d_{x,P}(\xi) \frac{\sum_{i=1}^n W \delta_{x,i}^2}{\delta_{x,P} \sum_{i=1}^n W \delta_{x,i}} \quad (1.3)$$

where $d_{x,P}$ is the finite horizontal displacement of a generic point P of the system and $\delta_{x,P}$ is its virtual horizontal displacement. For a given value of ξ , it is possible to define an equivalent period of vibration of the structure as:

$$T^*(\xi) = 2\pi \sqrt{\frac{d_x^*}{a^*}} \quad (1.4)$$

Since each structure is not rigid but has an elastic period of vibration (T_e), it follows that $T^*(\xi) \geq T_e$. Indeed, the capacity curve of the structure is defined as a bi-linear; the first section is defined by considering its elastic deformability while the second one is defined by considering its rigid block behaviour. The maximum displacement required by the structure for a given spectrum is defined as:

$$d_{\max}^* = \max(d_{xs}^*; d_{xs \max}^*) \quad (1.5)$$

where d_{xs}^* is the displacement demand obtained as the intersection between the capacity curve and the acceleration-displacement response spectrum and $d_{xs \max}^*$ is the maximum spectral displacement demand in the range $T_e \leq T^* < T_s^*$. In Figure 1 the procedure is shown relating to a single overturning rigid block. In this case, the rotation ϑ of the block around the point C may be assumed as generalized coordinate ξ .

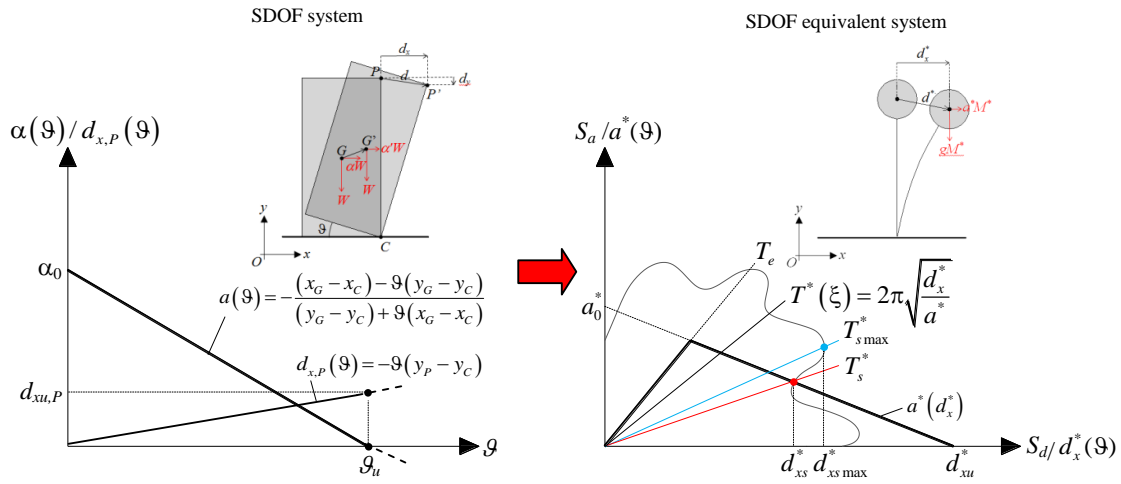


Figure 1. Scheme of the procedure of analysis

2. EXPERIMENTAL SET-UP

2.1. The arch model

The geometry of the model is depicted in Figure 2. The dimensions and proportions of the arch-pillar system have been defined by considering two complementary issues: standard rules of building art (Heyman, 1995); geometry of real historic masonry constructions (in particular, a standard cross section of a single nave church has been considered). Tie-rod is connected at the springings of arch.

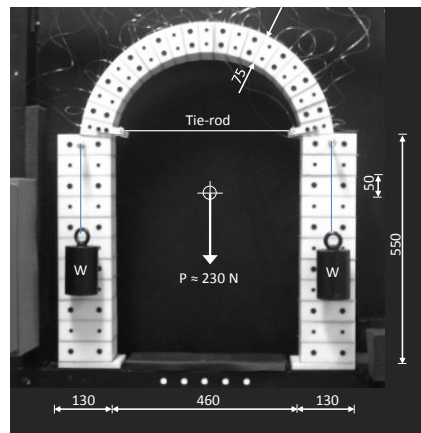


Figure 2. The arch model adopted: main features and dimensions

The model is composed of discrete blocks made of plastic material (11 for each pillar and 21 for the arch). Each block has been modelled by a numerical control machine (precision 1/10 mm). The plastic material adopted is a polymer named Polyamide 6 cast (PA 6 G). This choice derives from a compromise between stiffness, damage limitation, workability and hydro-thermal stability requirements. Stiffness was calibrated in order to let the theoretical hypothesis of rigid blocks be fulfilled and to guarantee the repeatability of the tests, thus minimizing damage to blocks due to impacts at collapse. In Table 1, mechanical properties of the material are reported.

Table 1. Arch parameters

PARAMETER	UNIT	MODEL VALUE	REF. VALUE
Specific weight of Polyamide 6 cast (p_{P6})	N/m ³	11500	-
Specific weight of PVA sheets (p_{PVA})	N/m ³	195÷390	-

Homogeneous specific weight (p_h)	N/m ³	~11430	21000 ⁽¹⁾
Modulus of elasticity of Polyamide 6 cast (E_{P6})	N/mm ²	1800÷3100	-
Modulus of elasticity of PVA sheets (E_{PVA})	N/mm ²	~275	-
Homogeneous modulus of elasticity (E_h)	N/mm ²	1750÷2940	1600 ⁽¹⁾
Compressive strength of blocks (f_c)	N/mm ²	60÷80	40 ⁽¹⁾
Span (s)	mm	550	5500
Friction coefficient	rad	0.6	0.7 ⁽¹⁾

¹Reference value for ancient brick masonry (NTC, 2008)

Due to the machine work of the blocks and the type of material adopted, the friction angle of the contact surfaces was very low (approximately 4°). In order to inhibit sliding, thin membranes of Polyvinyl Alcohol (PVA) foam 0.3 mm thick were introduced between blocks (Table 1). Such membranes allowed us to increase the friction coefficient up to 35°. Moreover, they provided the further advantage of reducing the edge effects on the corners of the blocks (the surface area of the membranes was slightly larger than that between blocks). However, it should be stated that membranes introduced a significant deformability to the arch-pillar system.

Two different tie-rods were considered in the arch-piers system. In Table 2, values of their mechanical properties are reported (some uncertainties are related to the evaluation of the effective section). Both tie-rods were subjected to an axial force of 10 N.

Table 2. Tie-rods parameters

PARAMETER	UNIT	STEEL	NYLON	REF. VALUE
Young modulus (E_t)	N/mm ²	67000	2840	206000 ⁽¹⁾
Ultimate elongation (ϵ_u)	%	0.046	0.189	0.04 ⁽¹⁾
Stress at failure (f_u)	N/mm ²	2800	780	500 ⁽¹⁾
Nominal diameter (d_t)	mm	0.2	0.3	40
Applied axial load (F)	N	10	10	10000 ⁽²⁾
Length (l)	mm	550	550	5500

¹Reference value for standard steel circular tie-rods, based on practical experience

²Typical value of axial load applied in the engineering practice

Despite the materials used and the scale reduction, the model is able to represent the main features of masonry arches. In particular, many theoretical and experimental studies (Heyman, 1995) have shown that their behavior mainly depends on the geometry of the system (shape and proportion) more than on their mechanical properties. Concerning the parameters, the main feature to be considered is the difference in stiffness and strength between blocks and joints. The use of quite rigid blocks with dry joints of soft material well represents it. In Table 3, similitude requirements are analyzed. It can be observed that they are only partially fulfilled by the model. In particular, in the model the arch-pillars-system should be more flexible and the tie-rods should be stiffer. Concerning the first aspect, it is worth noting that the elastic behaviour is attained only for very low actions, as small openings and sliding between blocks occur; thus, the actual deformability of the system is higher. Concerning the tie-rods, the paper aims to compare the effect of strengthening systems of different relative stiffness rather than their absolute values.

Table 3. Similitude requirements

PARAMETER	MODEL	REF. VALUE
$(p_h s)/E_h$	$\sim 2.86 \cdot 10^{-6}$	$72.2 \cdot 10^{-6}$
f_c/E_h	$\sim 3.05 \cdot 10^{-2}$	$2.50 \cdot 10^{-2}$
$(E_t d_t)/(E_h s)$	steel: $\sim 11.1 \cdot 10^{-3}$; nylon: $\sim 0.72 \cdot 10^{-3}$	$936 \cdot 10^{-3}$
$F/(p_h s^3)$	$5.25 \cdot 10^{-3}$	$2.86 \cdot 10^{-3}$

2.2. Experimental set-up and input

The tests have been performed at ENEA UTTMAT-QUAL laboratory, on a 2m x 2m 6-degree-of-freedom shaking table. The laboratory is equipped with a recently installed high resolution 3D motion capture system named 3DVision (Mongelli et al. 2010). It is a light-based system for 3D motion measurement exploiting a constellation of 9 near infrared (NIR) digital cameras for data acquisition and 4 DV cameras for synchronized movies. Retro-reflecting markers are positioned on the tested structure and their trajectory is reconstructed by spatial triangulation of NIR cameras rays. In the test series carried out on the arch, the displacements of 33 points were recorded. The acceleration of the shaking table and the stress in the tie-rods were monitored during each test as well.

The following four different arch configurations were considered: free standing arch (A); arch with steel tie-rod (B1); arch with nylon tie-rod (B2); arch with nylon tie-rod under asymmetric boundary conditions (C). Case C was obtained by fixing one of the pillars to the shaking table. Two different accelerograms (characterized by comparable PGAs and different displacement demands) were applied to each configuration. They were obtained by scaling two accelerograms recorded in L'Aquila 2009 earthquake (Figure 3). In particular, the time scale has been reduced by $\sqrt{10}$, in order to take into account the rigid block inelastic behaviour of the structure (see Figure 4, considering that the scale factor of the arch model is $\eta=10$).

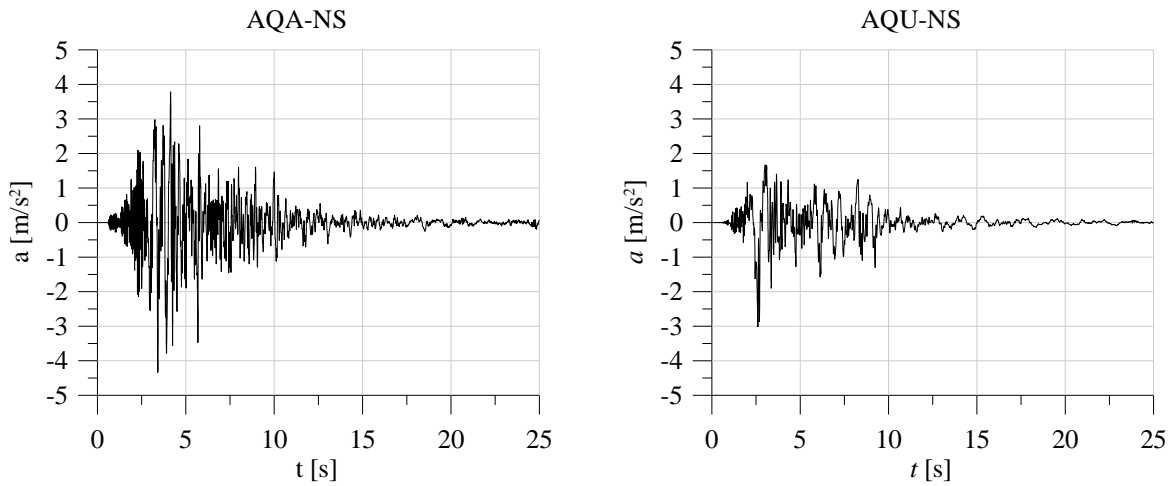


Figure 3. The real accelerograms considered in the test campaign

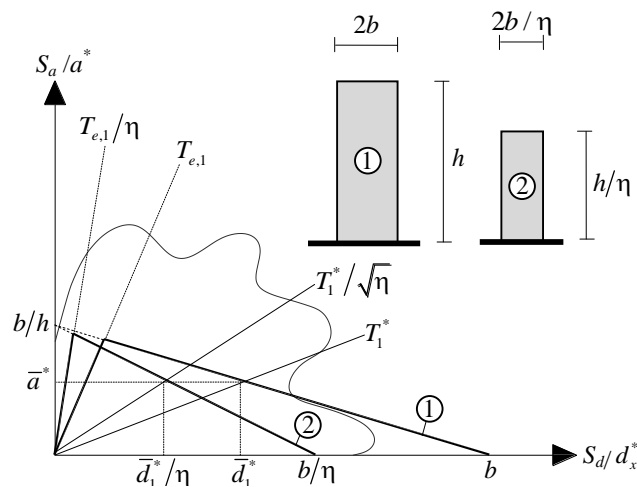


Figure 4. Scheme adopted for the time scale factor






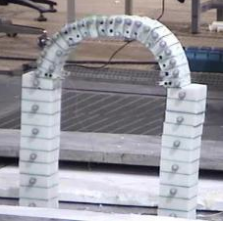


For each test configuration and each time-history the arch has been subjected to increasing value of

PGA up to collapse, thus performing an experimental Incremental Dynamic Analysis. The scale of accelerations have been modified in order to apply values of PGA proportional to the gravity acceleration. In order to be able to compare the experimental results with the theoretical ones, after the application of each time-history, the initial configuration of the arch was restored (by removing the residual relative displacements of the blocks that may have occurred during the test).

3. TEST RESULTS

In Table 4, the results of the test campaign are synthetized, for all the configurations considered, in terms of collapse PGA, collapse mode and maximum horizontal displacement at top of the piers. It can be observed that reinforced arches collapse for time-histories with PGA up to 6 times greater than free-standing arches. The collapse modes are different as well. In free standing arches, collapse is produced by the formation of 4 rotation hinges, typically 3 in the arch and 1 at the base of one pier (this latter collapsed only with AQU). In reinforced arches it is typically associated with sliding movements between the blocks. AQU input is more severe for the structure since it requires larger displacement capacity. The presence of more flexible tie-rods increases the displacement capacity of the structure and thus the collapse multiplier.

Table 4. Mechanisms, PGA and maximum displacement obtained in the test series.

Case	AQA	AQU
A: Free standing arch PGA Max Displacement	 0.50 g 66.48 mm (right pier)	 0.20 g Right pier collapsed
B1: Arch reinforced with rigid tie-rods PGA Max Displacement	 1.20 g 12.23 mm (left pier)	 1.00 g 35.32 mm (right pier)
B2: Arch reinforced with flexible tie-rods PGA Max Displacement	 2.00g 31.86 mm (left pier)	 1.30 g 53.58 mm (left pier)
C: Reinforced arch with flexible tie-rods and asymmetric b.c. PGA Max Displacement	 1.20 g 27.08 mm (right pier)	 0.85 g 35.02 mm (right pier)

In the following the entire set of time-history of the incremental dynamic analyses are analysed for the cases A and B1 only. In Table 5 the sequence of nominal PGAs of the time-histories applied to the systems are reported. In Figure 5, the spectral accelerations and displacement measured on the shaking table in correspondence of the collapse time-histories are depicted (damping is 5%). It can be observed that the input AQU, even with lower values of spectral acceleration, requires a larger displacement capacity of the structure.

Table 5. Sequence of time-histories applied to the configuration A and B1

PGA [g]	0.05	0.10	0.15	0.20	0.25	0.30	0.35	0.40	0.45	0.50	0.55	0.60	0.65	0.70	0.75	0.80	0.85	0.90	0.95	1.00	1.05	1.10	
	AQA																						
A	x		x	x	x	x	x	x	x	x													
B1								x	x	x	x	x	x	x	x	x	x	x	x	x	x	x	x
	AQU																						
A	x	x	x	x																			
B1									x	x	x	x	x		x						x		

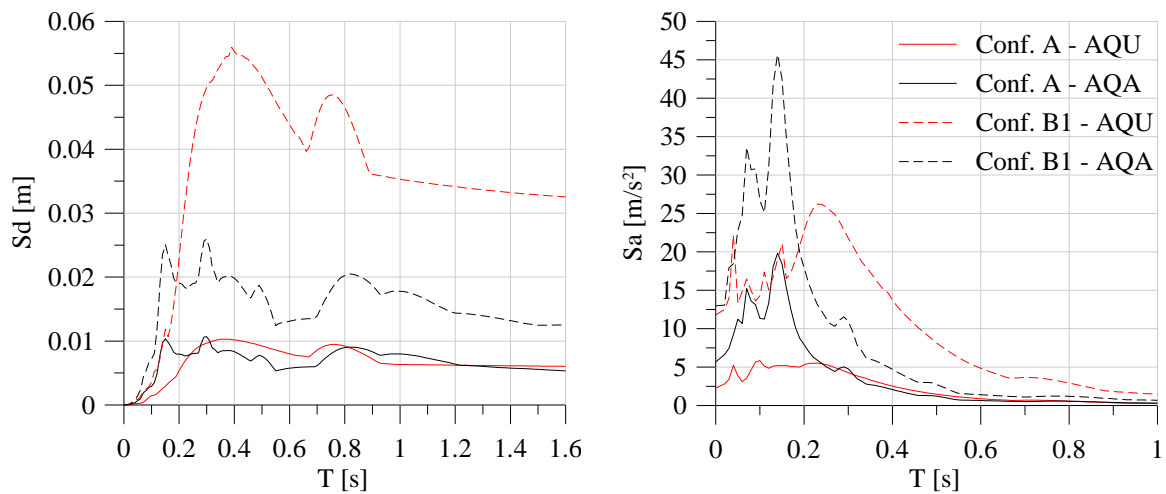


Figure 5. Acceleration and displacement spectra measured on the shaking table for free-standing arches (A)

In Figure 6 and 7, the input is represented in the spectral acceleration/displacement domain, together with the capacity curve of the structure calculated following the procedure illustrated in §1. For the free-standing arch (Figure 6) the capacity curve is defined on the basis of the mechanism depicted in Figure 8a. For the reinforced arch (Figure 7), two different capacity curves are represented: the blue one corresponds to that of Figure 8b - *4 hinges mechanism*, in which the tie-rod is modelled as a force whose value depends on F and on its increment related to the increasing of distance between point of applications; the red one corresponds to the mechanism illustrated in Figure 8b - *5 hinges mechanism*, in which the tie-rod is modelled as a rigid internal constraint. It can be observed that the acceleration value of activation of the 4-hinges mechanism is lower than the one related to the 5-hinges mechanism; this means that, at the beginning, 4 hinges appear in the system. However, the presence of the tie-rod opposes to the development of the mechanism and, before the yielding of the tie rod, the 5 hinges mechanism occurs. The slight slope of the dashed line indicates that the tie-rod is very flexible for this system, as already mentioned in § 2.1, commenting Table 3.

It can be observed that, in the arch configuration A (Figure 6), the intersection between the capacity curve and the spectral acceleration/displacement domain corresponding to pre-collapse input is approximately 25% of the maximum displacement capacity for AQA and 30% for AQU. Concerning the case B1 (Figure 7), the displacement corresponding to curve intersection is 17% of the maximum displacement for AQA and 36% for AQU.

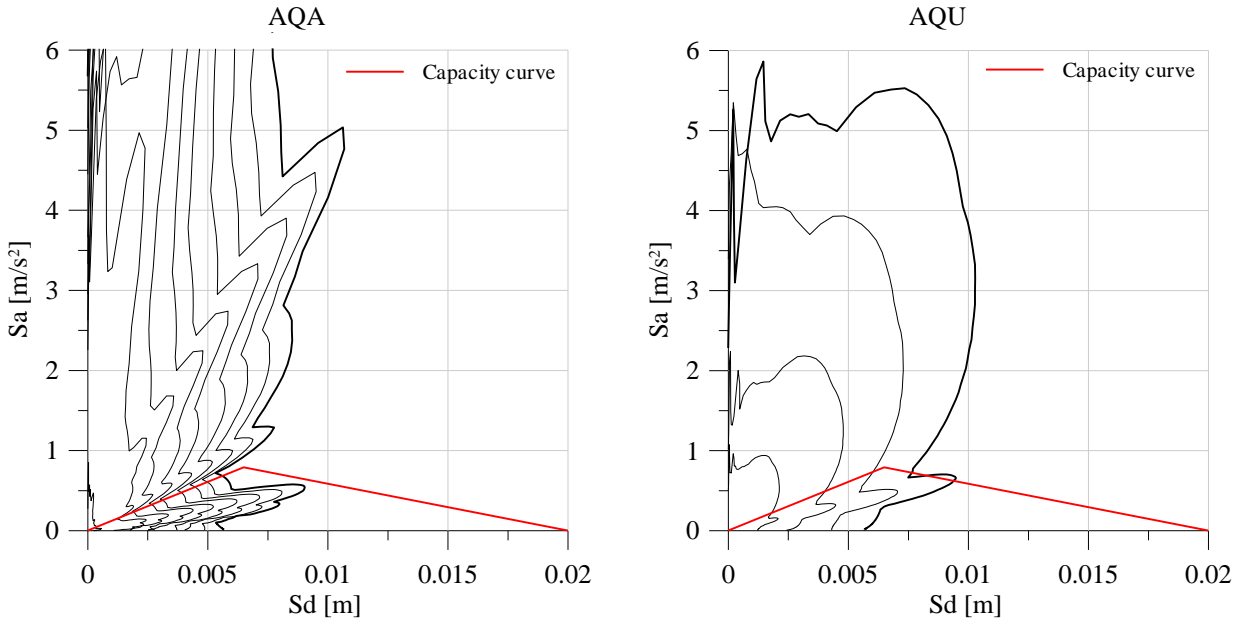


Figure 6. Acceleration/displacement spectra vs. capacity curve of free-standing arches (A)

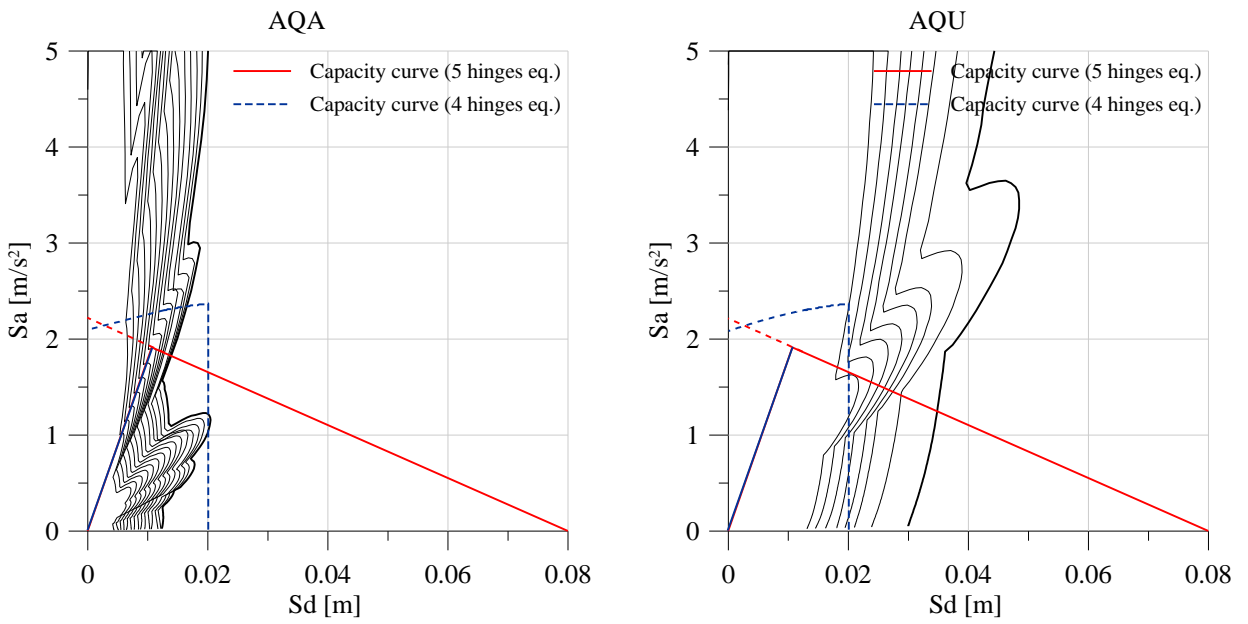


Figure 7. Acceleration/displacement spectra vs. capacity curve of reinforced arches (B1)

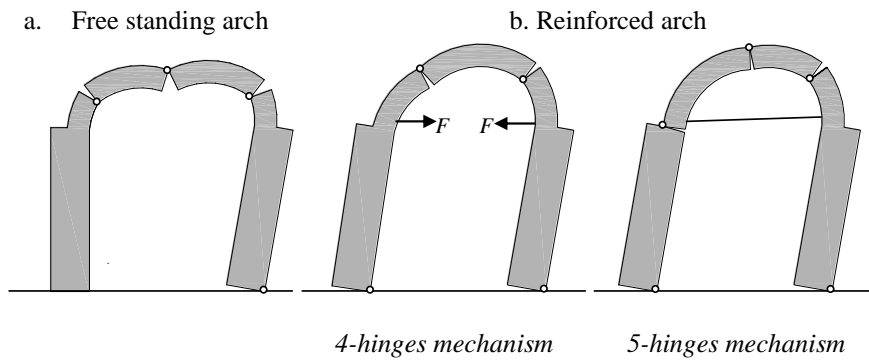


Figure 8. Mechanisms considered in the analyses

In Figure 9 and 10, the results of the experimental and theoretical incremental dynamic analysis are compared. For each time-history, the maximum horizontal displacement achieved on the top of the piers is plotted as a function of the nominal PGA applied. Moreover, the theoretical displacements calculated at the performance point and the maximum spectral displacement demand in the range $T_e \leq T^* < T_s^*$ are plotted. Both the cases show a great agreement between experimental and theoretical results. As regard the curves related to reinforced arch (Figure 10), it can be observed that there isn't a quick growing of the displacements in the displacements demand, as it occurs in the case of free standing arch, because the system is still far from the collapse.

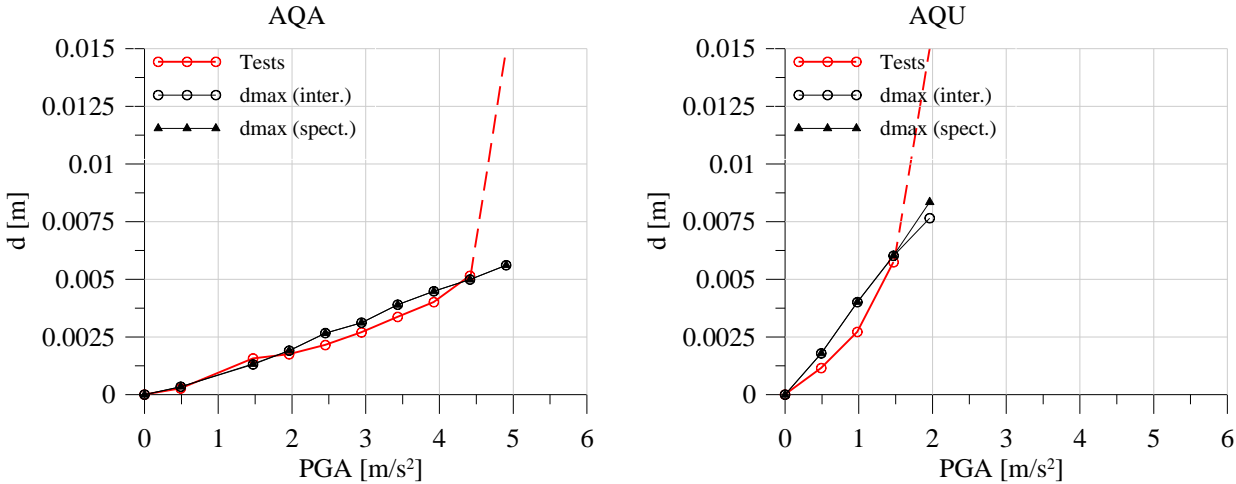


Figure 9. Incremental dynamic analysis of free-standing arches (A)

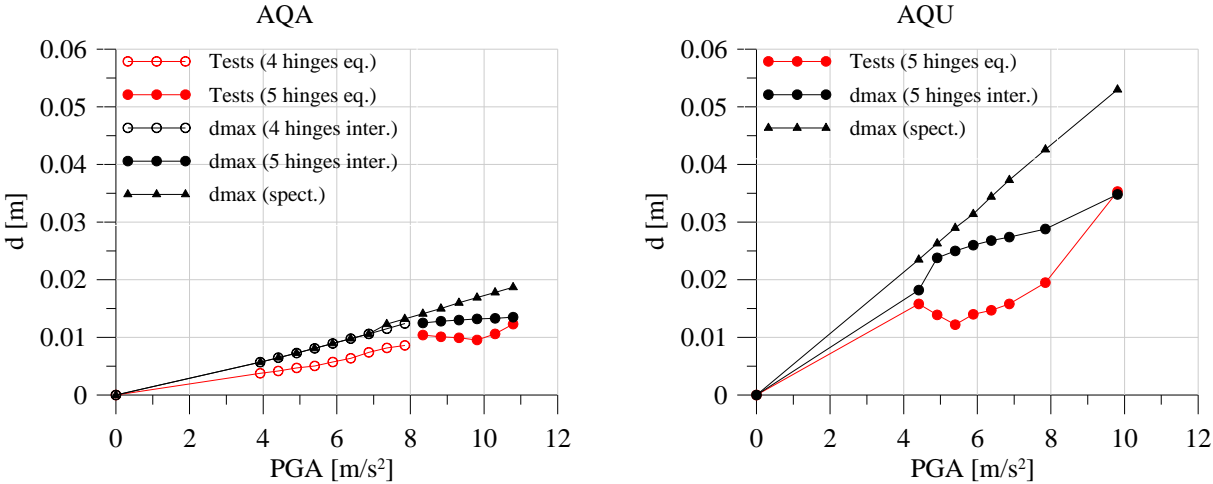


Figure 10. Incremental dynamic analysis of reinforced arches (B1)

4. CONCLUSIONS

Shaking table tests on a arch scale model, together with simple predicting models developed in the framework of displacement-based design methods, have been presented in this paper. Both free-standing and reinforced arch-piers systems were considered. The tests were performed by applying two different time-histories of increasing systems PGA (incremental dynamic analysis). From the experimental tests it was possible to observe that the acceleration leading to collapse free-standing arches is much lower than that of reinforced ones (up to 1/5). Different collapse modes were observed: for free standing arches, collapse was produced by the formation of rotation hinges (3 in the arch and 1 at the base of one of the piers), while for reinforced arches it was associated to sliding movements between of the blocks mainly. It has been assessed that the presence of more flexible tie-rods increases the

displacement capacity of the structure and thus the collapse multiplier. The interpretation of the results through simple analytical models led to a good agreement between the experimental and theoretical results. In particular, the comparison in terms of displacements showed the capability of the theoretical models to take into account the displacement capacity of the non-linear structure.

ACKNOWLEDGEMENT

The results have been achieved in the project PERPETUATE (www.perpetuate.eu), funded by the European Commission in the Seventh Framework Programme (FP7/2007-2013), under grant agreement n° 244229.

REFERENCES

- Heyman J. (1995). *The stone skeleton. Structural engineering of masonry architecture*, Cambridge University Press, Cambridge.
- Lagomarsino S., Resemini S. (2009). The Assessment of Damage Limitation State in the Seismic Analysis of Monumental Buildings. *Earthquake Spectra*, **25**: 2, pp. 323-346.
- Mongelli M., De Canio G., Roselli I., Colucci A., Tati A. (2010). 3D motion capture and FEM analysis for shaking table tests at ENEA Casaccia Research Center. Proc. 14 ECEE 2010, Ohrid, Macedonia.
- NTC, Norme Tecniche per le Costruzioni (2008). *Italian Building Code* (in Italian), D.M. 14/01/2008.